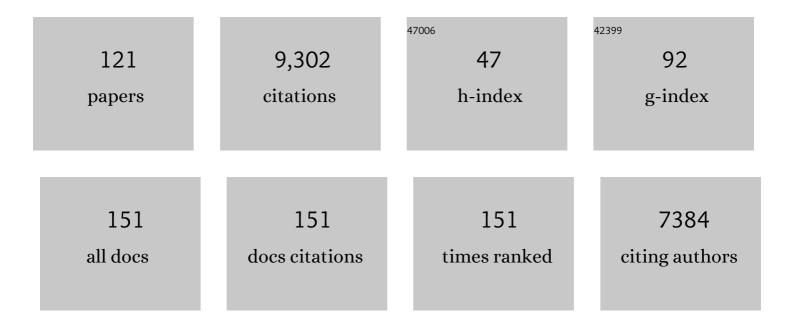
List of Publications by Year in descending order

Source: https://exaly.com/author-pdf/6997852/publications.pdf Version: 2024-02-01



#	Article	IF	CITATIONS
1	Modelling the mass budget and future evolution of Tunabreen, central Spitsbergen. Cryosphere, 2022, 16, 2115-2126.	3.9	0
2	Rapid fragmentation of Thwaites Eastern Ice Shelf. Cryosphere, 2022, 16, 2545-2564.	3.9	36
3	Brief communication: Thwaites Glacier cavity evolution. Cryosphere, 2021, 15, 3317-3328.	3.9	8
4	Two decades of dynamic change and progressive destabilization on the Thwaites Eastern Ice Shelf. Cryosphere, 2021, 15, 5187-5203.	3.9	22
5	An updated seabed bathymetry beneath Larsen C Ice Shelf, Antarctic Peninsula. Earth System Science Data, 2020, 12, 887-896.	9.9	8
6	The 2020 Larsen C Ice Shelf surface melt is a 40-year record high. Cryosphere, 2020, 14, 3551-3564.	3.9	16
7	Mass and enthalpy budget evolution during the surge of a polythermal glacier: a test of theory. Journal of Glaciology, 2019, 65, 717-731.	2.2	23
8	Impact of warming shelf waters on ice mélange and terminus retreat at a large SE Greenland glacier. Cryosphere, 2019, 13, 2303-2315.	3.9	26
9	Autonomous underwater vehicle (AUV) observations of recent tidewater glacier retreat, western Svalbard. Marine Geology, 2019, 417, 106009.	2.1	17
10	Monitoring Greenland ice sheet buoyancy-driven calving discharge using glacial earthquakes. Annals of Glaciology, 2019, 60, 75-95.	1.4	17
11	Calving controlled by melt-under-cutting: detailed calving styles revealed through time-lapse observations. Annals of Glaciology, 2019, 60, 20-31.	1.4	49
12	Dynamic vulnerability revealed in the collapse of an Arctic tidewater glacier. Scientific Reports, 2019, 9, 5541.	3.3	29
13	Physical Conditions of Fast Glacier Flow: 3. Seasonallyâ€Evolving Ice Deformation on Store Glacier, West Greenland. Journal of Geophysical Research F: Earth Surface, 2019, 124, 245-267.	2.8	13
14	Seawater softening of suture zones inhibits fracture propagation in Antarctic ice shelves. Nature Communications, 2019, 10, 5491.	12.8	11
15	A Full‣tokes 3â€Ð Calving Model Applied to a Large Greenlandic Glacier. Journal of Geophysical Research F: Earth Surface, 2018, 123, 410-432.	2.8	54
16	Tidewater Glacier Surges Initiated at the Terminus. Journal of Geophysical Research F: Earth Surface, 2018, 123, 1035-1051.	2.8	36
17	Reâ€assessment of the age and depositional origin of the Paviland Moraine, Gower, south Wales, <scp>UK</scp> . Boreas, 2018, 47, 577-592.	2.4	1
18	Decline in Surface Melt Duration on Larsen C Ice Shelf Revealed by The Advanced Scatterometer (ASCAT). Earth and Space Science, 2018, 5, 578-591.	2.6	30

#	Article	IF	CITATIONS
19	Multiple Late Holocene surges of a High-Arctic tidewater glacier system in Svalbard. Quaternary Science Reviews, 2018, 201, 162-185.	3.0	17
20	Intense Winter Surface Melt on an Antarctic Ice Shelf. Geophysical Research Letters, 2018, 45, 7615-7623.	4.0	65
21	Effects of undercutting and sliding on calving: a global approach applied to Kronebreen, Svalbard. Cryosphere, 2018, 12, 609-625.	3.9	29
22	Intercomparison and Validation of SAR-Based Ice Velocity Measurement Techniques within the Greenland Ice Sheet CCI Project. Remote Sensing, 2018, 10, 929.	4.0	18
23	Glacier Calving Rates Due to Subglacial Discharge, Fjord Circulation, and Free Convection. Journal of Geophysical Research F: Earth Surface, 2018, 123, 2189-2204.	2.8	26
24	What can knowledge of the energy landscape tell us about animal movement trajectories and space use? A case study with humans. Journal of Theoretical Biology, 2018, 457, 101-111.	1.7	13
25	Ice and firn heterogeneity within Larsen C Ice Shelf from borehole optical televiewing. Journal of Geophysical Research F: Earth Surface, 2017, 122, 1139-1153.	2.8	13
26	Extreme behavioural shifts by baboons exploiting risky, resource-rich, human-modified environments. Scientific Reports, 2017, 7, 15057.	3.3	42
27	The Impact of Föhn Winds on Surface Energy Balance During the 2010–2011 Melt Season Over Larsen C Ice Shelf, Antarctica. Journal of Geophysical Research D: Atmospheres, 2017, 122, 12,062.	3.3	39
28	Basal dynamics of Kronebreen, a fast-flowing tidewater glacier in Svalbard: non-local spatio-temporal response to water input. Journal of Glaciology, 2017, 63, 1012-1024.	2.2	31
29	Glacier Calving in Greenland. Current Climate Change Reports, 2017, 3, 282-290.	8.6	42
30	Rapidly changing subglacial hydrological pathways at a tidewater glacier revealed through simultaneous observations of water pressure, supraglacial lakes, meltwater plumes and surface velocities. Cryosphere, 2017, 11, 2691-2710.	3.9	49
31	Systems Analysis of complex glaciological processes and application to calving of Amery Ice Shelf, East Antarctica. Annals of Glaciology, 2017, 58, 60-71.	1.4	1
32	Structure and evolution of the drainage system of aÂHimalayanÂdebris-covered glacier, and its relationshipÂwithÂpatternsÂofÂmassÂloss. Cryosphere, 2017, 11, 2247-2264.	3.9	58
33	Observationally constrained surface mass balance of Larsen C ice shelf, Antarctica. Cryosphere, 2017, 11, 2411-2426.	3.9	16
34	Centuries of intense surface melt on Larsen C Ice Shelf. Cryosphere, 2017, 11, 2743-2753.	3.9	19
35	Melt-under-cutting and buoyancy-driven calving from tidewater glaciers: new insights from discrete element and continuum model simulations. Journal of Glaciology, 2017, 63, 691-702.	2.2	79
36	Stagnation and mass loss on a Himalayan debris-covered glacier: processes, patterns and rates. Journal of Glaciology, 2016, 62, 467-485.	2.2	109

#	Article	IF	CITATIONS
37	Annual down-glacier drainage of lakes and water-filled crevasses at Helheim Glacier, southeast Greenland. Journal of Geophysical Research F: Earth Surface, 2016, 121, 1819-1833.	2.8	29
38	Ocean forcing of glacier retreat in the western Antarctic Peninsula. Science, 2016, 353, 283-286.	12.6	346
39	Massive subsurface ice formed by refreezing of ice-shelf melt ponds. Nature Communications, 2016, 7, 11897.	12.8	63
40	Calving rates at tidewater glaciers vary strongly with ocean temperature. Nature Communications, 2015, 6, 8566.	12.8	214
41	Heterogeneity in Karakoram glacier surges. Journal of Geophysical Research F: Earth Surface, 2015, 120, 1288-1300.	2.8	119
42	Brief Communication: Newly developing rift in Larsen C Ice Shelf presents significant risk to stability. Cryosphere, 2015, 9, 1223-1227.	3.9	39
43	Seasonal dynamic thinning at Helheim Glacier. Earth and Planetary Science Letters, 2015, 415, 47-53.	4.4	31
44	Extensive retreat of Greenland tidewater glaciers, 2000–2010. Arctic, Antarctic, and Alpine Research, 2015, 47, 427-447.	1.1	63
45	The evolution of a submarine landform record following recent and multiple surges of Tunabreen glacier, Svalbard. Quaternary Science Reviews, 2015, 108, 37-50.	3.0	87
46	The glaciers climate change initiative: Methods for creating glacier area, elevation change and velocity products. Remote Sensing of Environment, 2015, 162, 408-426.	11.0	253
47	A new perspective on how humans assess their surroundings; derivation of head orientation and its role in †framing' the environment. PeerJ, 2015, 3, e908.	2.0	5
48	Glacier dynamics at Helheim and Kangerdlugssuaq glaciers, southeast Greenland, since the Little Ice Age. Cryosphere, 2014, 8, 1497-1507.	3.9	45
49	Brief Communication: On the magnitude and frequency of Khurdopin glacier surge events. Cryosphere, 2014, 8, 571-574.	3.9	37
50	Marine ice regulates the future stability of a large Antarctic ice shelf. Nature Communications, 2014, 5, 3707.	12.8	72
51	Surface melt and ponding on Larsen C Ice Shelf and the impact of föhn winds. Antarctic Science, 2014, 26, 625-635.	0.9	92
52	The structural and dynamic responses of Stange Ice Shelf to recent environmental change. Antarctic Science, 2014, 26, 646-660.	0.9	6
53	Modelling environmental influences on calving at Helheim Glacier in eastern Greenland. Cryosphere, 2014, 8, 827-841.	3.9	71
54	Marine ice formation in a suture zone on the Larsen C Ice Shelf and its influence on ice shelf dynamics. Journal of Geophysical Research F: Earth Surface, 2013, 118, 1628-1640.	2.8	43

#	Article	IF	CITATIONS
55	Satellite tracking large numbers of individuals to infer population level dispersal and core areas for the protection of an endangered species. Diversity and Distributions, 2013, 19, 834-844.	4.1	130
56	Glacier dynamics over the last quarter of a century at Helheim, Kangerdlugssuaq and 14 other major Greenland outlet glaciers. Cryosphere, 2012, 6, 923-937.	3.9	94
57	Basal crevasses in Larsen C Ice Shelf and implications for their global abundance. Cryosphere, 2012, 6, 113-123.	3.9	65
58	The response of Petermann Glacier, Greenland, to large calving events, and its future stability in the context of atmospheric and oceanic warming. Journal of Glaciology, 2012, 58, 229-239.	2.2	87
59	Integrated electrical resistivity tomography (ERT) and self-potential (SP) techniques for assessing hydrological processes within glacial lake moraine dams. Journal of Glaciology, 2012, 58, 849-858.	2.2	35
60	A Reconciled Estimate of Ice-Sheet Mass Balance. Science, 2012, 338, 1183-1189.	12.6	1,246
61	A rapidly growing moraine-dammed glacial lake on Ngozumpa Glacier, Nepal. Geomorphology, 2012, 145-146, 1-11.	2.6	75
62	Response of debris-covered glaciers in the Mount Everest region to recent warming, and implications for outburst flood hazards. Earth-Science Reviews, 2012, 114, 156-174.	9.1	449
63	A new 100-m Digital Elevation Model of the Antarctic Peninsula derived from ASTER Global DEM: methods and accuracy assessment. Earth System Science Data, 2012, 4, 129-142.	9.9	82
64	Dynamics of tidewater surge-type glaciers in northwest Svalbard. Journal of Glaciology, 2012, 58, 110-118.	2.2	46
65	Stable dynamics in a Greenland tidewater glacier over 26 years despite reported thinning. Annals of Glaciology, 2012, 53, 241-248.	1.4	10
66	Karakoram glacier surge dynamics. Geophysical Research Letters, 2011, 38, n/a-n/a.	4.0	167
67	Warming of waters in an East Greenland fjord prior to glacier retreat: mechanisms and connection to large-scale atmospheric conditions. Cryosphere, 2011, 5, 701-714.	3.9	93
68	Persistent iceberg groundings in the western Weddell Sea, Antarctica. Remote Sensing of Environment, 2010, 114, 385-391.	11.0	17
69	Present stability of the Larsen C ice shelf, Antarctic Peninsula. Journal of Glaciology, 2010, 56, 593-600.	2.2	52
70	Ocean regulation hypothesis for glacier dynamics in southeast Greenland and implications for ice sheet mass changes. Journal of Geophysical Research, 2010, 115, .	3.3	162
71	The location of the grounding zone of Evans Ice Stream, Antarctica, investigated using SAR interferometry and modelling. Annals of Glaciology, 2009, 50, 35-40.	1.4	21
72	Progress in satellite remote sensing of ice sheets. Progress in Physical Geography, 2009, 33, 547-567.	3.2	23

#	Article	IF	CITATIONS
73	Ice velocity and climate variations for Baltoro Glacier, Pakistan. Journal of Glaciology, 2009, 55, 1061-1071.	2.2	97
74	Englacial drainage systems formed by hydrologically driven crevasse propagation. Journal of Glaciology, 2009, 55, 513-523.	2.2	85
75	Surface structure and stability of the Larsen C ice shelf, Antarctic Peninsula. Journal of Glaciology, 2009, 55, 400-410.	2.2	84
76	A cut-and-closure origin for englacial conduits in uncrevassed regions of polythermal glaciers. Journal of Glaciology, 2009, 55, 66-80.	2.2	75
77	Hydrologic response of the Greenland ice sheet: the role of oceanographic warming. Hydrological Processes, 2009, 23, 7-30.	2.6	110
78	Quantification of Everest region glacier velocities between 1992 and 2002, using satellite radar interferometry and feature tracking. Journal of Glaciology, 2009, 55, 596-606.	2.2	166
79	Airborne SAR monitoring of tree growth in a coniferous plantation. International Journal of Remote Sensing, 2008, 29, 3873-3889.	2.9	8
80	Observations of forest stand top height and mean height from interferometric SAR and LiDAR over a conifer plantation at Thetford Forest, UK. International Journal of Remote Sensing, 2007, 28, 1173-1197.	2.9	39
81	Positive mass balance during the late 20th century on Austfonna, Svalbard, revealed using satellite radar interferometry. Annals of Glaciology, 2007, 46, 117-122.	1.4	16
82	DEM quality assessment for quantification of glacier surface change. Annals of Glaciology, 2007, 46, 189-194.	1.4	18
83	Early recognition of glacial lake hazards in the Himalaya using remote sensing datasets. Global and Planetary Change, 2007, 56, 137-152.	3.5	252
84	Modeling the refreezing of meltwater as superimposed ice on a high Arctic glacier: A comparison of approaches. Journal of Geophysical Research, 2007, 112, .	3.3	44
85	Improvement of Satellite Radar Feature Tracking for Ice Velocity Derivation by Spatial Frequency Filtering. IEEE Transactions on Geoscience and Remote Sensing, 2007, 45, 2309-2318.	6.3	38
86	Acceleration in thinning rate on western Svalbard glaciers. Geophysical Research Letters, 2007, 34, .	4.0	166
87	The potential of satellite radar interferometry and feature tracking for monitoring flow rates of Himalayan glaciers. Remote Sensing of Environment, 2007, 111, 172-181.	11.0	129
88	Fine-resolution remote-sensing and modelling of Himalayan catchment sustainability. Remote Sensing of Environment, 2007, 107, 430-439.	11.0	15
89	Rapid and synchronous ice-dynamic changes in East Greenland. Geophysical Research Letters, 2006, 33, .	4.0	184
90	Modelling the impact of superimposed ice on the mass balance of an Arctic glacier under scenarios of future climate change. Annals of Glaciology, 2005, 42, 277-283.	1.4	22

4

#	Article	IF	CITATIONS
91	Glacier surge dynamics of Sortebræ, east Greenland, from synthetic aperture radar feature tracking. Journal of Geophysical Research, 2005, 110, .	3.3	73
92	Seasonal variation in velocity before retreat of Jakobshavn Isbræ, Greenland. Geophysical Research Letters, 2005, 32, .	4.0	104
93	Classification of forest volume resources using ERS tandem coherence and JERS backscatter data. International Journal of Remote Sensing, 2004, 25, 751-768.	2.9	33
94	The 1999 and 2000 eruptions of Mount Cameroon: eruption behaviour and petrochemistry of lava. Bulletin of Volcanology, 2003, 65, 267-281.	3.0	136
95	Estimation of tree growth in a conifer plantation over 19 years from multi-satellite L-band SAR. Remote Sensing of Environment, 2003, 84, 184-191.	11.0	26
96	Urban building height variance from multibaseline ERS coherence. IEEE Transactions on Geoscience and Remote Sensing, 2003, 41, 2022-2025.	6.3	15
97	Is there a single surge mechanism? Contrasts in dynamics between glacier surges in Svalbard and other regions. Journal of Geophysical Research, 2003, 108, .	3.3	166
98	ERS SAR feature-tracking measurement of outlet glacier velocities on a regional scale in East Greenland. Annals of Glaciology, 2003, 36, 129-134.	1.4	32
99	Surge-related topographic change of the glacier Sortebræ, East Greenland, derived from synthetic aperture radar interferometry. Journal of Glaciology, 2003, 49, 381-390.	2.2	16
100	Surge potential and drainage-basin characteristics in East Greenland. Annals of Glaciology, 2003, 36, 142-148.	1.4	62
101	The initiation of glacier surging at Fridtjovbreen, Svalbard. Annals of Glaciology, 2003, 36, 110-116.	1.4	45
102	Ice dynamics during a surge of Sortebræ, East Greenland. Annals of Glaciology, 2002, 34, 323-329.	1.4	32
103	Accuracy assessment of a large-scale forest cover map of central Siberia from synthetic aperture radar. Canadian Journal of Remote Sensing, 2002, 28, 719-737.	2.4	32
104	Blue Reflectance Provides a Surrogate for Latewood Density of High-Latitude Pine Tree Rings. Arctic, Antarctic, and Alpine Research, 2002, 34, 450.	1.1	42
105	Surface flow evolution throughout a glacier surge measured by satellite radar interferometry. Geophysical Research Letters, 2002, 29, 10-1-10-4.	4.0	237
106	Glacier motion estimation using SAR offset-tracking procedures. IEEE Transactions on Geoscience and Remote Sensing, 2002, 40, 2384-2391.	6.3	490
107	Blue Reflectance Provides a Surrogate for Latewood Density of High-latitude Pine Tree Rings. Arctic, Antarctic, and Alpine Research, 2002, 34, 450-453.	1.1	103

Deriving forest characteristics using polarimetric InSAR measurements and models., 2001,,.

#	Article	IF	CITATIONS
109	Repeat-Pass Interferometric Coherence Measurements of Disturbed Tropical Forest from JERS and ERS Satellites. Remote Sensing of Environment, 2000, 73, 350-360.	11.0	33
110	Tropical Forest Biomass Density Estimation Using JERS-1 SAR: Seasonal Variation, Confidence Limits, and Application to Image Mosaics. Remote Sensing of Environment, 1998, 63, 126-139.	11.0	144
111	Repeat-pass interferometric coherence measurements of tropical forest from JERS and ERS satellites. , 1998, , .		3
112	Texture in airborne SAR imagery of tropical forest and its relationship to forest regeneration stage. International Journal of Remote Sensing, 1997, 18, 1333-1349.	2.9	39
113	A study of the relationship between radar backscatter and regenerating tropical forest biomass for spaceborne SAR instruments. Remote Sensing of Environment, 1997, 60, 1-13.	11.0	215
114	Exploratory study of the relationship between tropical forest regeneration stages and SIR-C L and C data. Remote Sensing of Environment, 1997, 59, 180-190.	11.0	60
115	Familiar face recognition: A comparative study of a connectionist model and human performance. Neurocomputing, 1995, 7, 3-27.	5.9	17
116	Modelling Peripheral Pre-Attention And Foveal Fixation For Search Directed Machine Vision Systems. Proceedings of SPIE, 1990, 1197, 99.	0.8	0
117	A Real-Time Image Acquisition And Processing System For A RISC-Based Microcomputer. Proceedings of SPIE, 1989, , .	0.8	0
118	A simple model for the estimation of biomass density of regenerating tropical forest using JERS-1 SAR and its application to Amazon region image mosaics. , 0, , .		0
119	Mapping deforestation in Amazon with ERS SAR interferometry. , 0, , .		4
120	Biomass estimation of Thetford forest from L-band SAR data: potential and limitations. , 0, , .		1
121	Introducing a landcover map of Siberia derived from MERIS and MODIS data. , 0, , .		2